Heliyon 9 (2023) e16534

Contents lists available at ScienceDirect

Heliyon

journal homepage: www.cell.com/heliyon

Research article

Shock absorption capability of corrugated ring yield mount subjected to high impact loading

Shahbaz Khan, Muhammad Shahiq, Muhammad Zahid Iqbal *

Department of Mechanical Engineering, Pakistan Institute of Engineering and Applied Sciences Islamabad (PIEAS), Pakistan

ARTICLE INFO

Keywords:
Energy absorbing device
Impact loading
Shock absorption
Shock test
AutoDyn

ABSTRACT

Various types of mechanical energy-absorbing devices are known that operate by plastic deformation. The corrugated ring mount that is used in this study relates to a device that absorbs energy by plastic deformation. This energy-absorbing device has reduced volumetric proportions, simple in design, and therefore has small overall dimensions and can be mass-produced at low cost. This study aims to determine the shock absorption capability and efficiency of this mount against impact loading. For this, Finite Element Method Analysis (FEA) and experimentation are done. The FEA is done using the Explicit Dynamics (AutoDyn) module of ANSYS Workbench and for experimentation Drop Test Machine (DTM) is used. In this study impact load from low g up to 85 g is applied and a very close agreement is found between FEA and experimental results. There is just a 5–10% deviation between the findings. The results show that this mount is plastically deformed to absorb the impact energy with a maximum efficiency of 70%. It concludes that it is a reliable and safer shock energy device.

1. Introduction

Shock is a force acting for a very short span of time, usually less than one natural time period of the system to which it is applied [1]. Mechanical shock may be defined as a sudden change in velocity and is a major design consideration for a wide variety of systems and their components [2]. Example of shocks are earthquake, underwater explosion and pyro-shock. Shock is the vector quantity, and it has same unit, as of acceleration and its standard unit is 'g' (1 g = 10 m/s^2). The forces involved in forge hammers, punch presses, blasts, and explosions are examples of shock load. In this study, pulse shock is used which is a force or acceleration profile, applied in the form of half sine wave. Shock isolation is the phenomena of reducing the effects of shock. The shock isolators store the energy just like the electrical energy stored by a capacitor, and then release it over a longer duration. Shock isolation is a daunting task and damping devices are required to isolate the shock's propagation from the source to the target. The usual shock mounts absorb low g impact but for high g impact (above 60 g) requires special devices. Yield mount(s) is the type of shock damper that detach the high shock's transmission to the target from source.

The yield mount converts impact kinetic energy to strain energy that allows it to yield. The factors that affect the working of yield mounts are: the method and magnitude of applied load, deformation/displacement pattern, transmission rate, and material properties. These mounts are mostly metal and are used only once.

Dynamic response of parts/systems under impact loading is an important topic in applied engineering. Dynamic loading in Military

* Corresponding author.
E-mail address: muhammad_zi@pieas.edu.pk (M.Z. Iqbal).

https://doi.org/10.1016/j.heliyon.2023.e16534
Received 13 October 2022; Received in revised form 17 May 2023; Accepted 18 May 2023
Available online 23 May 2023

and commercial equipment like Submarines, Mobiles, Laptops Automobiles needs to be analyzed critically. An FEA can easily be used to predict the dynamics of a system affectively.

Ansys AudoDyn can be used quickly to simulate large material deformation during failure under impact loading. It has a range of models to represent the complex physical phenomenon as a result of interaction of solids, liquids and gases. The blast for precision mining, automobile crash cases, underwater explosions and many similar high impact dynamics cases can be studied.

The research on shock-absorbing devices dates back to WWI. During this time, shock testing began in the form of underwater explosions and study of its effects on ships and submarines. In WWII, a series of equipment/materials failures occurred due to shock propagation. Therefore, researchers felt the importance of shock damping devices to prevent the structure's damage [3]. Later on, a lot of damping devices were invented that were used for shock absorption while preventing the target body from being damage.

Makai et al. [4] for automobiles invented a plastically deformable piston-cylinder type of shock absorbing device. Nishimura et al. [5] invented bellows/tubes type of impact absorbing device for vehicles. Mire [6] invented a corrugated metal tube type yield mount. Bergey et al. [7] gave an idea of a rectangular sheet having non-isotropic properties that are employed in vehicle seats for reducing the acceleration or deceleration effects on the occupants. Sicking [8] innovates the tube-folding energy absorber. When impact forces applied to it, this absorber fold and compress the tube. Olabi et al. [9] gave an overview of tube-type energy absorbers. Choi et al. [10] studied the various combinations of mild steel tubes used in high-speed highways. These tubes are mainly made up of ductile material and plastically deformed after the application of impact load. Yazici et al. [11] study the effects of impact loading on mechanical properties of steel fiber reinforced concrete. Lei et al. [12] analyzed the performance of building using wedge devices in the steel structure. Salehghaffari et al. [13] performed numerous efforts to increase the shock damping feature of circular metallic tubes. Jotepaa et al. [14] tested the high shock up to 50 g for designing the hybrid micro circuit (HMCs) that are used in defense and aerospace industries. Leblouba et al. [15] improves the shock and vibration isolation of an elliptical leaf spring used in structure and equipment. Siam [16] established a reliable and efficient shock simulation method using FEA to analyze the high shock effects in space structures. Teruna et al. [17] checked the response of various steel dampers in the structure in case of an earthquake. Iqbal et al., [18] used the drop test machine to study the various types of shock pulses that are generated by the rubber wave generator.

There are many shapes of yield mounts like tubular shapes, J type mounts [20], frusta, struts, sandwich plates, and some other special shapes such as honeycomb cells and stepped circular thin walls tube [21]. A variety of mechanical energy-absorbing devices are known that works on the principle of plastic deformation. But all these known devices involve the combination of a number of elements and therefore their shapes correspond to substantial volumetric proportions that make them difficult to handle. Also, their cost is also relatively high.

The previous work gives an information about various types of mounts and their applications. The literature discussed also gives clear specifications for different types of mounts. However, not so much research is carried out to evaluate the mounts response against static and dynamic loading. There is no particular literature available on the experimental and theoretical study of these types of energy absorbers subjected to yield loadings. This study maps out the mount behavior when subjected to impact loadings. Shock pulse is applied, and the mount response is analyzed both numerically and experimentally. Additionally, efficiency and reliability of the mount is also rated under extreme impact load. Moreover, shock is the vector quantity, and it has same unit as of acceleration. The unit *g* represents the multiple of acceleration of gravity. The 85 g shock means the acceleration of 85 times of *g* is produced when impact load is applied.

In this study, corrugated ring mount [6] is used that is scale down to lab scaled for shock absorption study. The shock is given to the mount by dropping it from certain height. This mount absorbs the shock by plastically deforming itself, preventing the source body from damage and it has outer diameter of 100 mm and 1 mm thickness which means it can be easily installed in compact space even for the high shock (up to 85 g). It also has simple design, of reduced volumetric proportions, and it can be mass-produced at a relatively low cost.

This mechanical absorbing device comprises a metal plate having a plurality of lateral fastening points around its periphery and a central fastening point. This metal plate consists of a series of a repeated patterns, the slots of one series being angularly shifted about those of the adjacent series and gradually shorter from outwards towards the center. Hence, because of this type of arrangement the metal plate comprises distortion bridges located between the slot of each series [6].

The amount of energy absorbed by the corrugated ring mount depends upon the nature of the metal plate, thickness, the number of slots per series, the width and length of these slots, relative spacing, and a number of the series of slots. When this metal plate is subjected to the load, then the central fastening point displaces with respect to said lateral fastening point. The amount of shock being absorb depends on how much the central fastening point is displaced as compared to the lateral fastening point.

This study has these main steps.

i. Analysis of the metal mount using the Finite Element method. For the FEA, Explicit Dynamics (AutoDyn) module of ANSYS Workbench is used. The FEA is done, by giving the velocity profile at the lateral fastening point of the mount. Mesh independence is also performed to check the proper convergence of the solution.
ii. Experimentation of the mount using a drop test machine. In DTM, mount is installed on the drop table, and this is dropped at the certain height. The accelerometers are used for measuring of shock profile. Above the base table of the DTM, Rubber wave Generator (RWG) is attached for generating the sinusoidal shock pulse. The equipment is placed on the rigid ground to prevent the unnecessary vibrations.
iii. Shock profile, Shock transmits and deformations from FEA and experimentation are compared.

The limitations of this mount/study are that mount used for the analysis is for once time use only. It has to be replaced after

Table 1
Properties of Material Used to manufacture Corrugated Mount.

	Properties (Standard)	UTM Test (ASTM A370)
Material	Galvanized Steel - G01	
Reference Standard	ISO3573-96	
Elastic Modulus (E) (GPa)		190
Yield Strength (MPa)	260	260
Tensile Strength (MPa)	410	490
C (%age)	0.1	0.09
Poisson Ratio		0.33

application of impact load. Also, the material used for the mount is steel and based on this material, it has the ability to absorb shock up to 85 g. Beyond this point, the mount will be fractured, and concept of energy absorption under plastic deformation will be faded away.

2. Finite element analysis of metal mount

For FEA analysis of corrugated ring mount, explicit dynamic solver is used. The equation that is used for studying the non-linear motion at each node is [22].

$$\boldsymbol{M}\ddot{d} + f_{int}(d) = f_{ext} \tag{1}$$

In the above Equation (1), M is the mass matrix, d is nodal displacement, f_{int} is internal forces and f_{ext} is external forces. The nodal displacement at each time step is given by Equation (2)

$$d_{t+\Delta t} = 2d_t - d_{t-\Delta t} + \Delta t^2 m^{-1}(f_{ext} - f_{\text{int}}(d)) \tag{2}$$

The accuracy of the explicit method depends on the time step size. Smaller the step size, better results could be obtained. According to Courant-Friedrichs-Lewy (CFL) condition, the time-step is limited so that a stress wave cannot travel further than the smallest element characteristics length in a single time step. The step can be formulated by following Equation (3):

$$\Delta t \leq f\left[\frac{h}{c}\right] \tag{3}$$

Where.

h: characteristics length of a finite element (average dimension of element)
c: wave speed in the material (depends on the material)
f: safety factor, $f \leq 1$

The minimum time step in any explicit analysis should be equal or less than the value finds from the above equation. It shows that minimum characteristic length is controlling the time step size in explicit analysis, therefore element size should be as uniform as possible in one simulation [23] [24]. There is longitudinal and transverse wave in the material as previous one is much faster than latter one therefore time step is controlled by longitudinal wave speed. The longitudinal elastic wave can be calculated by young modulus and density. It can be calculated by following Equation (4)

$$c = \sqrt{\frac{E}{\rho}} \tag{4}$$

In this study, minimum time step is 1.28×10^{-7} s and total analysis time is 20msec, so the number of time steps require for this analysis is 15.62×10^4.

The material properties are used that are obtained from tensile and composition testing. These properties are shown in Table 1. Like the steel mount used in this study have an elastic modulus of 190 GPa, yield strength of 260 MPa and ultimate tensile strength of 490 MPa, having a 0.09% of carbon composition. No heat treatment, strain hardening, or surface improvement process are done on the material. The boundary conditions are applied according to the requirement. For studying the plastic range of the material, the Bilinear Isotropic Hardening model is used, and apply the Plastic Strain model having maximum equivalent plastic strain of 0.3 for studying the failure of the material.

At the four bolts of the ring, the shock is produced, and its acceleration profile was created using half sin waveform. The basic governing Equation (5) of this waveform is given below [24].

$$a_s(t) = a_o \sin\left(\frac{\pi t}{\Gamma}\right) \quad 0 \leq t \leq \Gamma \tag{5}$$

Where:
a_o is the shock's amplitude

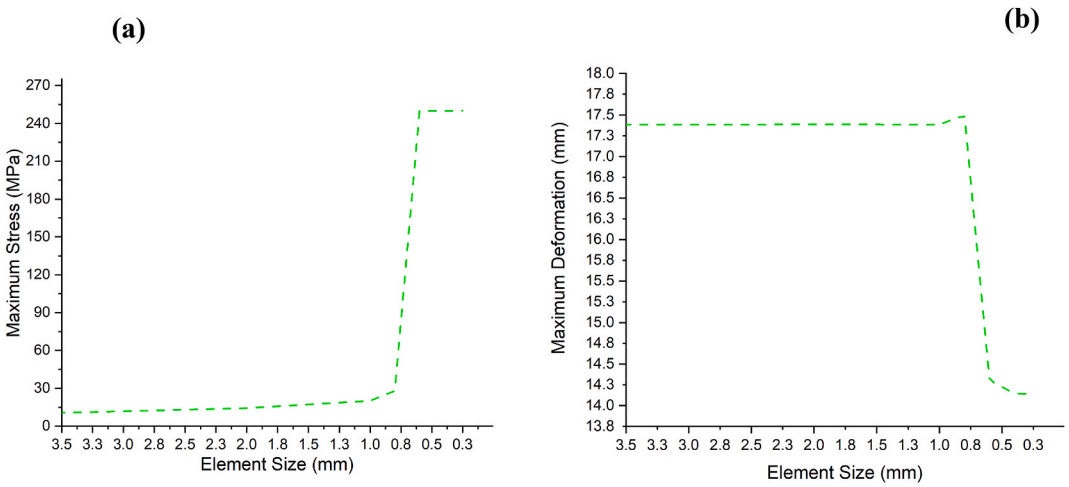

Fig. 1. Mesh independence analysis - element size plot (a) maximum stress plot (b) maximum deformation plot.

Fig. 2. Structured Mesh of the mount.

Table 2
Different meshing parameters.

	Element Quality	Aspect Ratio	Jacobian	Skewness
Minimum	0.52817	1.0137	0.40244	0.00083
Maximum	0.99988	2.8205	0.99982	0.83426
Average	0.94583	1.3540	0.93656	0.07833

Γ is shock load duration

This acceleration profile is converted into velocity by using the trapezoidal rule and this velocity is then applied to the four lateral fastening points of the corrugated ring mount. The trapezoidal rule is the numerical method of finding the exact value of definite integral. When this integral is performed on the acceleration, it gives the velocity profile. At the central fastening point of the mount, the weight of 2 kg is installed. The mesh independence for the mount is shown in Fig. 1.

The graphs of mesh independence show that when element size decreases then more realistic results are obtained. When it is less than 1 mm (thickness of mount) then the solution converges for a higher value of stress and lesser value of deformation. From 0.8 mm to 0.25 mm, there is almost no as a such change in results, although computational time increases exponentially by decreasing element size below 0.5 mm. So, for the analysis the 0.65 mm element size is used having total 35,436 elements that give better results at an optimum computational time. Also, the hex element is used which has a greater number of nodes as compared to the tri element. The

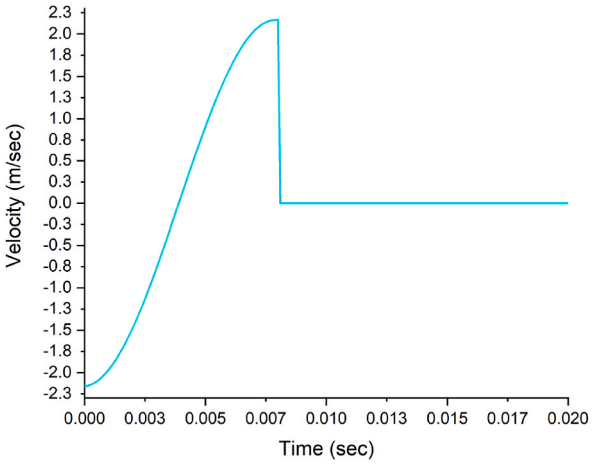

Fig. 3. Velocity profile at lateral fastening point of the mount.

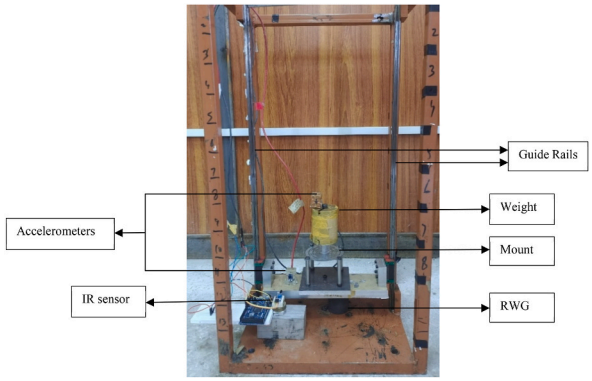

Fig. 4. Drop test machine.

model of the corrugated ring mount having structured mesh is shown in Fig. 2.

Element type and size are selected in such a way that it gives realistic results. Here, the multizone method is used along with the element's sizing. The multizone method gives automatic decomposition of geometry into free (unstructured) and mapped (structured) regions. This method meshed all regions with pure hexahedral elements. If hex mesh is not possible, free mesh will be generated in unstructured region. Others parameters like Jacobian, aspect ratio, material's behavior and skewness etc. are also being checked for getting the mesh independence. The different parameter's value for this mesh is given in Table 2.

Initially, the maximum velocity for the given case is given to the mount and weight attached at the central fastening point. At the four lateral fastening points of the mount around its periphery, a velocity profile is applied that is obtained by applying the trapezoidal rule on the shock profile. Fig. 3 shows the velocity profile.

3. Experimental setup

For the experimentation of corrugated ring yield mount, DTM is used. The mount is installed on the drop table and at the periphery four bolts are used for lateral fastening and at the central fastening, the weight of 2 kg is installed. Two accelerometers (one installed at the drop table and the other directly onto the mass) having a sensitivity of 2.15 mV/g are used for determining the shock applied and shock transmitted profile respectively. The IR sensor is installed along the drop table just to actuate the accelerometer for taking the reading. All these sensors are processed by the Arduino Due controller.

3.1. Drop test machine

Tests are performed on DTM shown in Fig. 4 at various heights to observe shock pulses. The IR sensor is installed on the base plate, and it actuates when the drop table passes through it. When the drop table crossed it, the IR triggers and once this turns on then accelerometers begin to take a reading during this time interval [18] [25]. It is important to mention that all the items during the test are installed rigidly so that load distribution is as uniform as possible. Any non-uniform load distribution may affect the slides motion

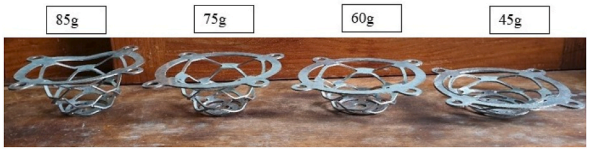

Fig. 5. Mounts subjected to impact loadings.

Table 3
Summary of the four experiments of impact loadings with mass at center of 2 kg.

Test No	Profile(g)	Drop Height (mm)	Applied (g)		Transmitted (g)		Displacement (mm)		Efficiency (%)		Highest Stress (MPa)
			Exp	FEA	Exp	FEA	Exp	FEA	Exp	FEA	
01	45	305	43.99	44.98	18.68	13.27	11.7	13.748	57.5	70.4	286.09
02	60	508	60.14	59.98	21.05	16.90	22.30	25.754	64.4	71.89	373.96
03	75	610	74.97	73.25	24.24	17.34	27.70	28.512	67.6	76.3	394.25
04	85	610+Initial Jerk	85.16	84.97	25.90	23.82	28.6	32.325	69.58	71.96	441.85

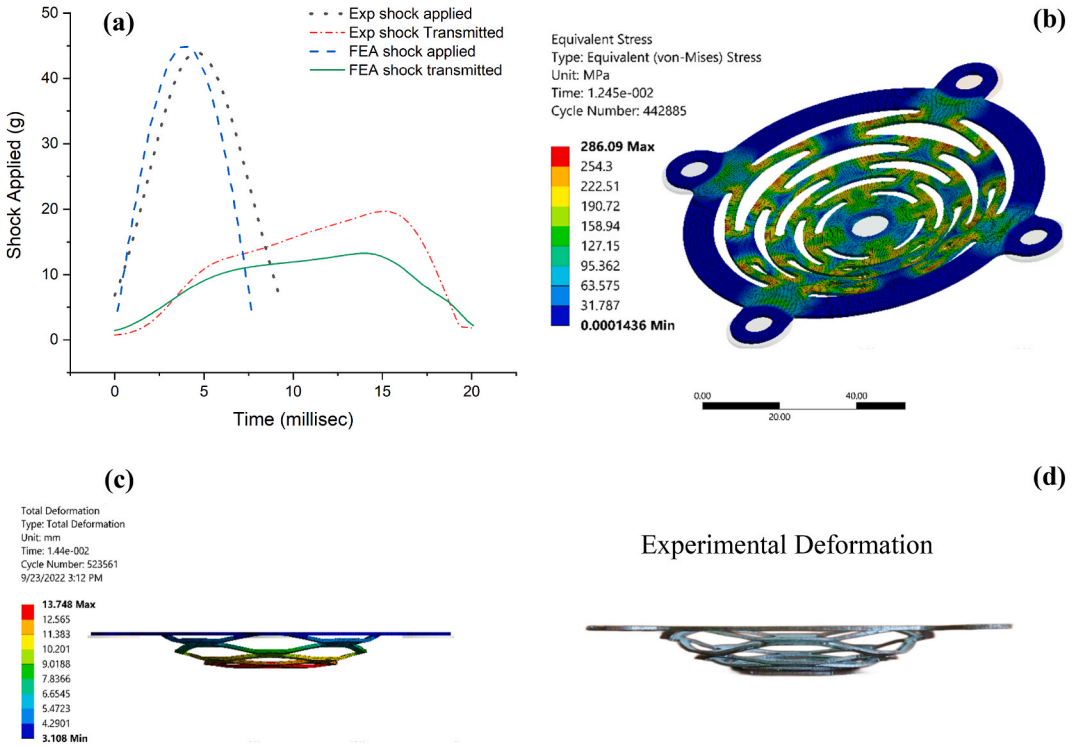

Fig. 6. Analysis at 45 g Shock: (a) 45 g shock profile, (b) Equivalent Stress value at 45 g shock, (c) Total Deformation value using FEA at 45 g shock, (d) Experimental Deformation value at 45 g shock.

and also increases the friction as well. The accelerometers are also installed firmly to the drop table and mount central fastening point because looseness in them may not be able to take shock profile correctly. Above the base table, RWG is installed that is used for generating sinusoidal shock pulse [25]. The data acquisition from these sensors (like accelerometers, and IR) is done by Arduino DUE. It is recommended that the measured shock pulse should pass through a low pass filter having a bandwidth of at least 5*X* the frequency of the shock pulse that is being generated.

The accelerometer attached to the surface of the Drop table acquires the applied shock profile. The corrugated mount is subjected to this shock waveform from drop table. 2nd accelerometer attached to the weights acquires the shock transmitted. This 2nd profile of the shock from weights is the value which the mount has not absorbed. The shock load can be integrated over time to give overall effect [19]. However due to severeness of the impact loading at high values, peak values are considered important in impact loading. Considering the peak values of the shock, the shock absorption efficiency can be defined as following Equation (6):

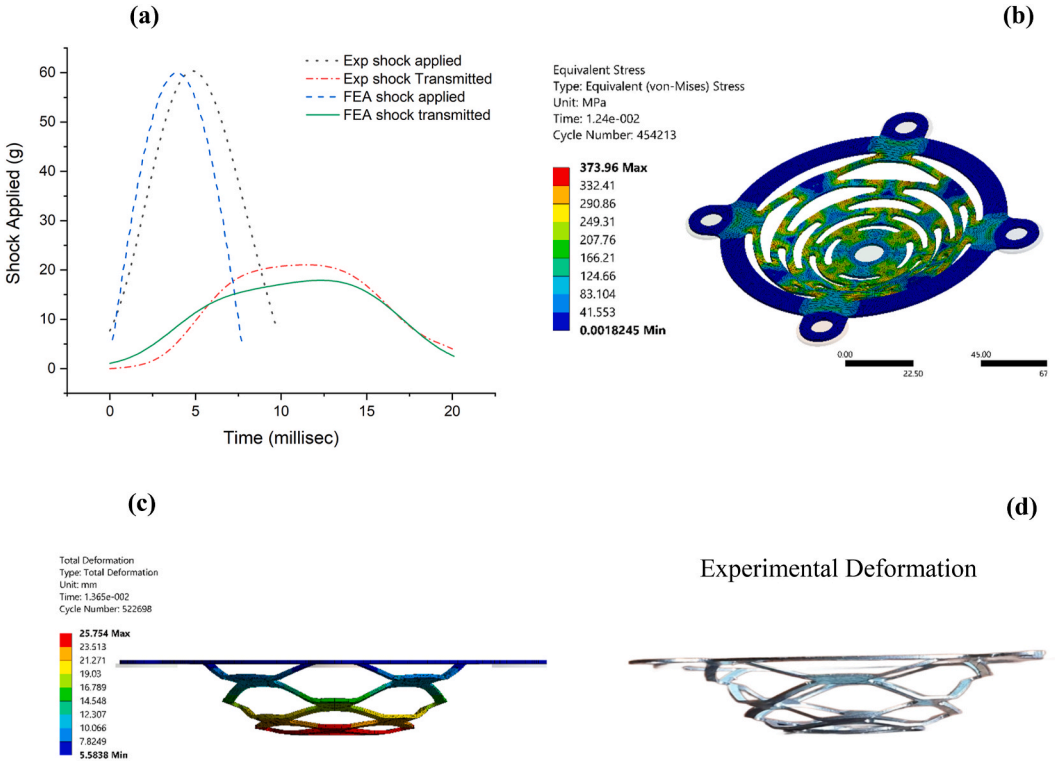

Fig. 7. Analysis at 60 g Shock: (a) 60 g shock profile, (b) Equivalent Stress value at 60 g shock, (c) Total Deformation value using FEA at 60 g shock, (d) Experimental Deformation value at 60 g shock.

$$Efficiency = 1 - \frac{Shock\ Transmitted}{Shock\ Applied} \tag{6}$$

Where Shock Transmitted is the Max. shock Transmitted and shock applied is the maximum value of shock applied. It is ratio of difference between shock applied and transmitted to the shock applied. In this study, the corrugated ring mount is used against impact loading. At the lateral fastening points (that are four in numbers), the shock is applied by dropping the drop table from certain height and at the central fastening point of the mount, shock transmitted is calculated.

4. Results and discussions

The analysis is done using 2 kg of weight at the center of the mount. An optimum value of weight of 2 kg is selected after few analysis and experimental tests. At lower weights, shock absorption efficiency is not good. At high value of weight, the mount breaks out. An optimum value of weight gives us a guideline to install the number of mounts on a particular structure. A heavy structure requires a greater number of mounts to be installed in parallel.

Fig. 5 shows the distorted Mounts subjected to different shock profiles. These mounts are subjected to 45, 60, 75 and 85 g sinusoidal shock pulses. The results are summarized in Table 3.

First test is carried out using DTM at a drop height of 305 mm giving a 45 g sinusoidal shock. The plot in Fig. 6 shows the shock applied and transmitted on the corrugated mount. The shock profile has a time period of 8 msec and reaches the maximum amplitude around 3.5–4.4 msec while transmitted shock gives its response after some delay of 2–3 msec and then reaches its peak value around 12–16 msec and after this, it dampens to zero. The transmitted shock for FEA has less amplitude of around 12 g while for experimentation it has around 19 g. The maximum stress value of the mount at this shock load is 286.09 MPa. This value depicts that the mount is permanently deformed because the yield point is 260 MPa and the highest stress value is greater than this point. The deformation value for 45 g shock in both FEA and experimentation are 13.74 mm and 11.70 respectively.

Fig. 7 shows plots for 60 g shock profile. This value of shock is obtained when table is dropped from the 508 mm height. The difference in shock transmitted amplitude in FEA and experimentation is less as compared to 45 g shock pulse. This is due to dominance of frictional losses at low shock. Moreover, the transmitted shock amplitude in experimentation is around 19 g while in FEA it has an amplitude of almost 16 g which depicts the small difference in the efficiency of the mount in experimentation and FEA. Also, both in FEA and experimentation the transmitted shock damps to zero after 16 msec. The stress value for this shock load is 373.96Mpa which shows that the mount is in the plastic region and permanently deformed. The deformation value for 60 g shock in both FEA and experimentation are 25.75 mm and 22.30 mm respectively.

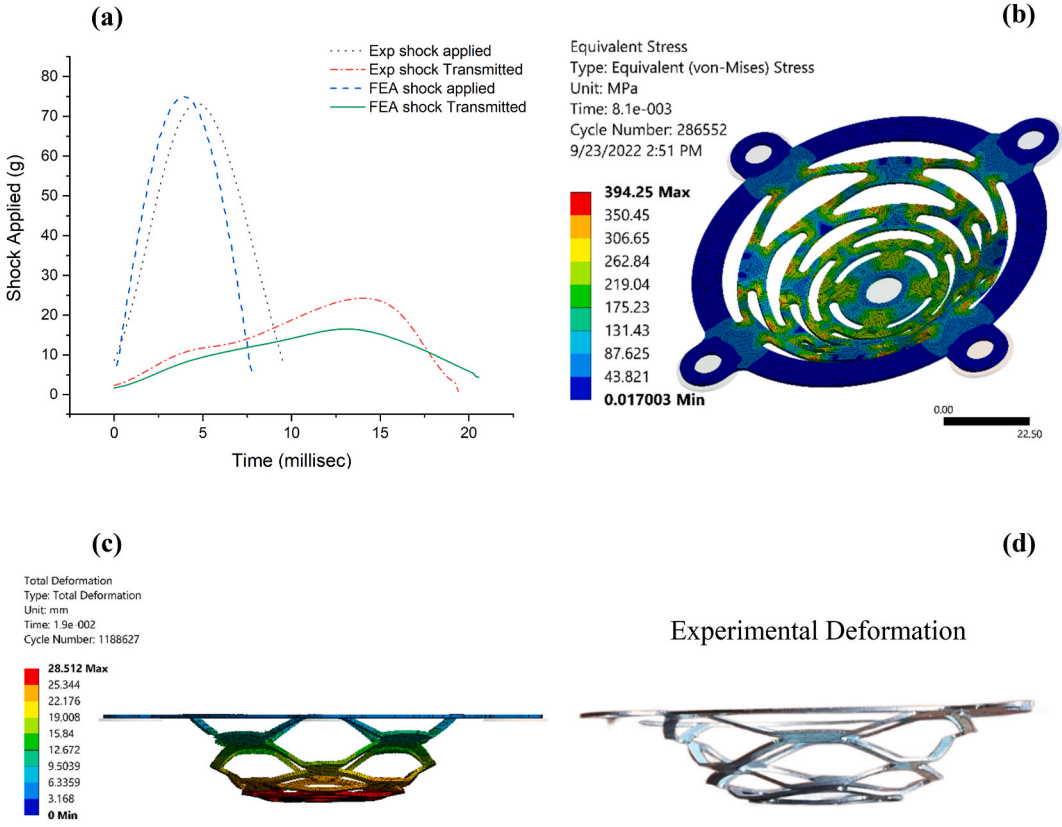

Fig. 8. Analysis at 75 g Shock: (a) 75 g shock profile, (b) Equivalent Stress value at 75 g shock, (c) Total Deformation value using FEA at 75 g shock, (d) Experimental Deformation value at 75 g shoc0k.

Fig. 8 shows plots for 75 g profile. In the experimentation, the 75 g shock value is obtained when DTM table is dropped from 610 mm height. There is a small difference in amplitude of shock produced in FEA and experimentation and both reaches their peak value around 4 msec. Also, the applied shock profile is for 8msec for both cases. The transmitted shock in FEA has an amplitude of 15 g (peak value) while in experimentation it has an amplitude of 22 g, so in FEA it has more efficiency as compared to experimentation because frictional effects during shock transmission are not considered. On the other hand, during FEA system is more rigid and has symmetrical loading but, in the experimentation, system may have some flexibility and unbalance mass distribution resulting in non-symmetric yielding and deterioration of results. Also, the peak value of shock in FEA and experimentation is obtained around 14–16 msec and after this time both are damped to zero. The highest stress value for this impact load is 394.25 MPa which shows that the mount has crossed its elastic limit and it is now in plastic domain. Also, the maximum stresses produced at the distortion bridge (distance among slots of each series) of the corrugated ring mount. The deformation value for 75 g shock in both FEA and experimentation are 28.51 mm and 27.70 mm respectively.

Fig. 9 shows plots for 85 g shock profile. To get the higher value of shock applied, the DTM table is fallen from 610 mm height with jerk. The Drop Machine (DTM) has a height of maximum 24 inches, therefore, to have a higher value of impact, it is given some initial velocity [18]. An initial jerk is given to the drop table to get a higher value of impact. The FEA and experimentation profile of applied shock is almost same having total time duration of almost 8msec. The transmitted shock reaches the maximum amplitude of 21 g and 25 g in both FEA and experimentation respectively. Due to frictions among various components in experimentation, the experimental shock transmitted is less compared to FEA.

The maximum stress value for the mount at this shock load is 441.85Mpa which is much greater than yield point but less than ultimate tensile strength point. It means that for this impact load the mount is plastically deformed but not fractured. The deformation value for 85 g shock in both FEA and experimentation are 32.32 mm and 28.60 mm respectively.

The stresses produced Fig. 11 in the corrugated ring mount for different impact load depicts that for each case it is greater than 260 MPa (yield point of the material). Greater the stresses produce; more will be the deformation in the mount as shown in Fig. 10. As for 45 g, the highest stress value is 286 MPa which means that mount is plastically deformed, and it has deformed value of 13.74 mm. For 60 g shock, the maximum stresses produce is 373.96 MPa with FEA deformation value of 25.75 mm. Similarly, the stresses produce for 75 g shock is 394.25 MPa with the deformation of 28.51 mm. For the last case (85 g shock), the 441.85 MPa stress is produced along with deformation of 32.32 mm. In the nutshell, it is observed that by increasing impact load there will be more shock absorption, more energy absorption, along with increase in deformation having greater value of maximum stress for increasing impact load.

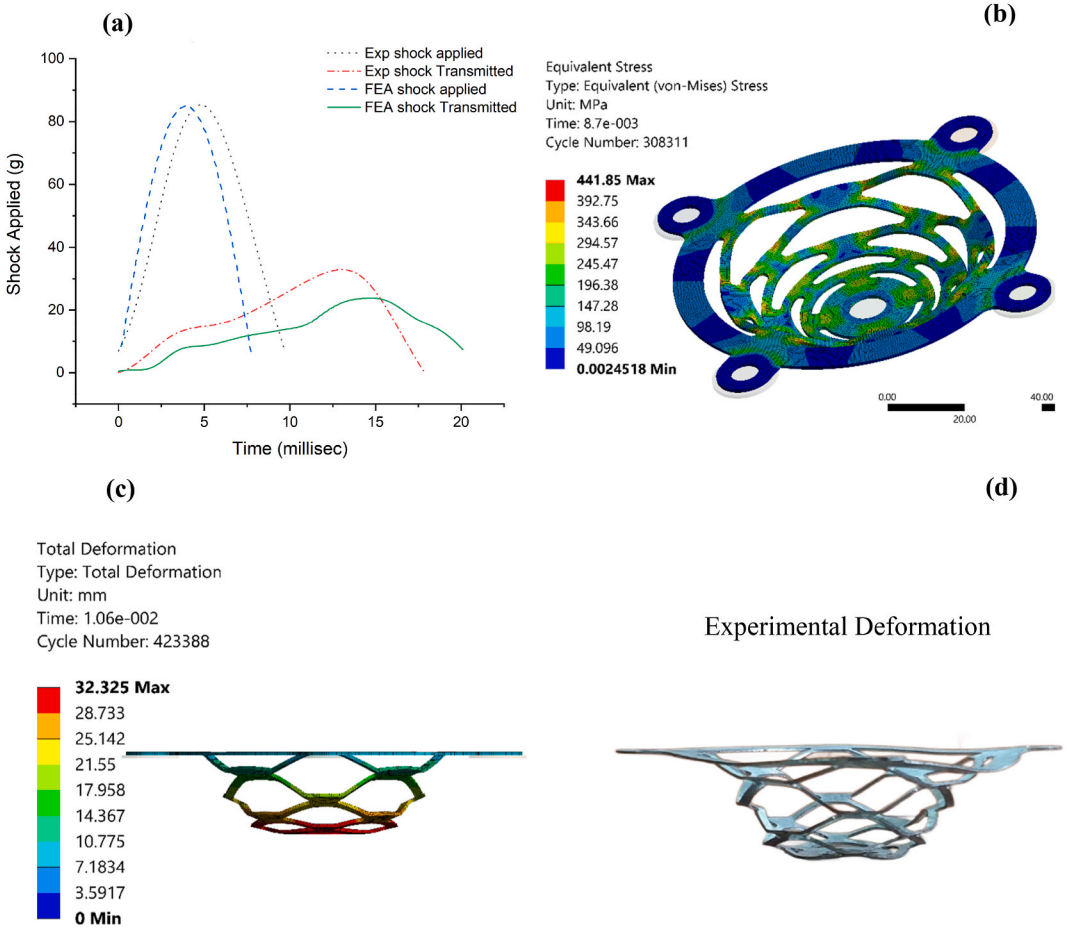

Fig. 9. Analysis at 85 g Shock: (a) 85 g shock profile, (b) Equivalent Stress value at 85 g shock, (c) Total Deformation value using FEA at 85 g shock, (d) Experimental Deformation value at 85 g shock.

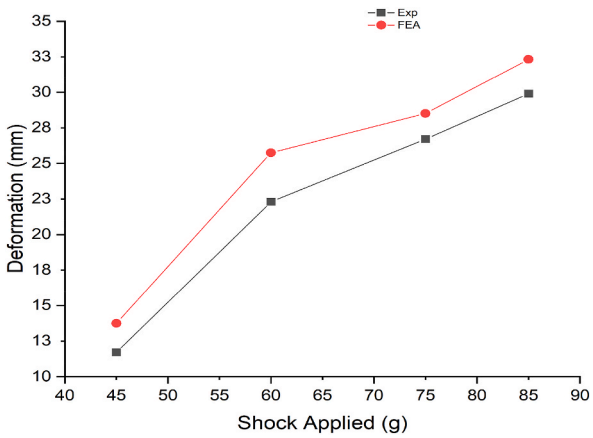

Fig. 10. Deformation comparisons.

The efficiency plot shown in Fig. 12 shows that it has efficiency of around 70%. For low impact load, mount is less efficient, but its efficiency increases for higher impact. Energy absorption in plastic mode is maximum when the plastic deformation process participation time is maximum. If the greater percentage of shock period undergo elastic deformation, the energy absorption will be quiet less. Therefore, at a low value of impact, there is more percentage of time for elastic deformation resulting in lower energy absorption

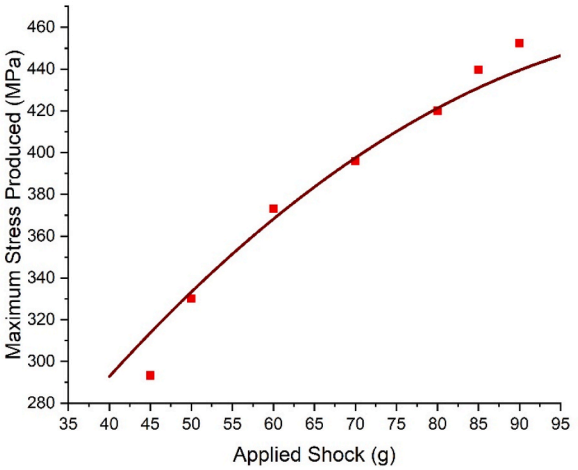

Fig. 11. Maximum Stress produced at various shock.

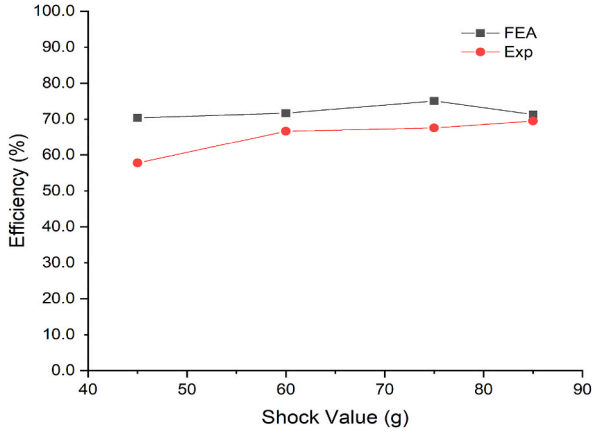

Fig. 12. Efficiency at various Shock.

efficiency compared to higher efficiency at higher value of shock due to greater percentage of time period for plastic deformation. This results in increase of efficiency with the increase of shock. This can also be observed in Fig. 11, which shows greater stress produced at higher value of g/shock. However, if the shock is increased beyond certain limits, the efficiency will decrease. This phenomenon is due to the fracture of the mount at higher value of shock. Therefore, there is an optimum value of shock (75 g) at which efficiency is maximum. It is therefore, to obtain the best efficiency of these type of yielding mounts, these should be loaded with an optimum weight to produce enough plastic deformation under a particular shock pulse.

As mount has more efficiency in FEA as compared to experimentation so it means there will be more deformation in previous vis a vis latter one and this is also validated by the graph as well because more shock absorption takes place in FEA as compared to experimentation. The reason for this difference is the friction effects and other uncertainties in experimentation.

5. Conclusion

The shock absorption capability of a corrugated ring mount is determined both by FEA and experimentation. The custom materials properties are used that were obtained from tensile and composition testing. For the FEA, mesh independence is done, then boundary conditions are applied according to the requirements. Deformation, stress, shock applied and transmitted are obtained. In the experimentation, the test was performed from low g up to 85 g with a few kg of weight at its center. However, both in FEA and experimentation, the pulse shape is almost the same for shock applied and shock transmission with a difference of 5–10%. The shock applied has a pulse duration of 8 msec and shock transmission peaks occur around 14–16msec after this it damp to zero up to 20msec. The Shock absorption efficiency found to be 70% for higher values of g. Max value of shock absorption efficiency is obtained at a shock level of 75 g. Above all, it is concluded that this corrugated ring mount has better shock absorption capability, and it can sustain the impact up to 85 g without being fractured.

Data availability

The Data that support the results in this study can be found from the corresponding author on request.

Declaration of competing interest

The authors declare that they have no known competing financial interests or personal relationships that could have appeared to influence the work reported in this paper

Acknowledgments

The authors also wish to thank PIEAS, Islamabad for using of lab facilities and financial support.

References

[1] S.S. Rao, Mechanical Vibration, Addison-Wisley Publishing Company, 2000.
[2] J.E.J.S. Alexander, vibration, Shock response spectrum-a primer 43 (6) (2009) 6–15.
[3] C. Lalanne, Mechanical Shock, John Wiley & Sons, 2014.
[4] S. Maki, Y. Nishimura, A. Fujiki, Shock Absorbing Device, Google Patents, 1969.
[5] Y. Nishimura, M. Okino, Impact Absorbing Means for Vehicles, Google Patents, 1970.
[6] N. Le Mire, Plastic Deformation-Absorbing Devices, Google Patents, 1971.
[7] K.H. Bergey, Energy-absorbing Aircraft Seat, Google Patents, 2003.
[8] D. Sicking, Systems and Methods for Absorbing Energy, Google Patents, 2015.
[9] A.-G. Olabi, E. Morris, M.J. T.-w. s. Hashmi, Metallic tube type energy absorbers: a synopsis, Thin-Walled Struct. 45 (7–8) (2007) 706–726.
[10] S.T. Choi, J.F. Carney, J.R. Veillette, Energy-dissipation characteristics of steel tubes, Exp. Mech. 26 (1986) 301–305, https://doi.org/10.1007/BF02320142.
[11] S. Yazici, H.S. Arel, V. Tabak, The effects of impact loading on the mechanical properties of the SFRCs, Construct. Build. Mater. 41 (2013) 68–72, https://doi.org/10.1016/j.conbuildmat.2012.11.095.
[12] J.S. Lei, W.X. Luo, J.L. Jiang, W. Zhang, Seismic performance analysis of steel frame with wedge devices based on the energy dissipation, Appl. Mech. Mater. 580 (2014) 1624–1628, https://doi.org/10.4028/www.scientific.net/amm.580-583.1624. Trans Tech Publications Ltd.
[13] S. Salehghaffari, M. Tajdari, M. Panahi, F. Mokhtarnezhad, Attempts to improve energy absorption characteristics of circular metal tubes subjected to axial loading, Thin-Walled Struct. 48 (6) (2010) 379–390, https://doi.org/10.1016/j.tws.2010.01.01.
[14] Santosh Joteppa, Vinod S. Chippalkatti, Design and qualification of hybrid micro circuit packages for higher vibration loads for aerospace and defense application, Int. J. Aero. Sci. 2 (3) (2013) 106–123, https://doi.org/10.5923/j.aerospace.20130203.04.
[15] Moussa Leblouba, Salah Altoubat, Muhammad Ekhlasur Rahman, Balaji Palani Selvaraj, Elliptical leaf spring shock and vibration mounts with enhanced damping and energy dissipation capabilities using lead spring, Shock Vib. (2015), https://doi.org/10.1155/2015/482063. Article ID 482063, 12 pages.
[16] N. Siam, in: Development of an Efficient Analysis Method for Prediction and Structural Dimensioning of Space Structures Subjected to Shock Loading, 2010.
[17] Daniel R. Teruna, Taksiah A. Majid, Bambang Budiono, Experimental study of hysteretic steel damper for energy dissipation capacity, Adv. Civ. Eng. (2015), https://doi.org/10.1155/2015/6317256. Article ID 631726, 12 pages.
[18] Muhammad Zahid Iqbal, Asif Israr, To predict a shock pulse using non linear dynamic model of rubber waveform generator, Int. J. Impact Eng. 147 (2021), 103731, https://doi.org/10.1016/j.ijimpeng.2020.103731.
[19] Y. Shimazaki, S. Nozu, T. Inoue, Shock-absorption properties of functionally graded EVA laminates for footwear design, Polym. Test. 54 (2016) 98–103, https://doi.org/10.1016/j.polymertesting.2016.04.024.
[20] M. Shahiq, M.Z. Iqbal, FEA Analysis of a J-type Yielding Mount, 2016 International Conference on Emerging Technologies (ICET), 2016, pp. 1–4, https://doi.org/10.1109/ICET.2016.7813233.
[21] A.A.A. Alghamdi, Collapsible impact energy absorbers: an overview, Thin-Walled Struct. 39 (2) (2001) 189–213, https://doi.org/10.1016/S0263-8231(00)00048-3.
[22] A. El-Zafrany, Non-linear finite element analysis of solids and structures: volume 2: advanced topics, Proc. Inst. Mech. Eng. 211 (6) (1997) 489.
[23] Ansys Autodyn, Interactive Non-linear Dynamic Analysis Software, Version 12, User's Manual, SAS IP Inc, 2009.
[24] Lixin Xu, Yiyuan Li, Jianhua Li, Chongying Lu, Mechanical response of MEMS inductor with auxiliary pillar under high-g shock, Micromachines 9 (4) (2018) 176, https://doi.org/10.3390/mi9040176.
[25] Muhammad Zahid Iqbal, Asif Israr, Tanveer Abbas, Semi Active Control of sinusoidal shock waveform on drop test machine (DTM) using non-linear dynamic model of hybrid wave generator (HWG) consisting of rubber and electromagnet, Rev. Sci. Instrum. 94 (3) (2023), 35005, https://doi.org/10.1063/5.0124138.